Original Paper

Skin Pharmacology and Physiology

Skin Pharmacol Physiol 2012;25:200–207
DOI: 10.1159/000338538

Received: January 12, 2012
Accepted after revision: March 14, 2012
Published online: May 16, 2012

Study of the Influence of the Penetration Enhancer Isopropyl Myristate on the Nanostructure of Stratum Corneum Lipid Model Membranes Using Neutron Diffraction and Deuterium Labelling

T.N. Engelbrecht[a] B. Demé[b] B. Dobner[a] R.H.H. Neubert[a]

[a]Institute of Pharmacy, Martin Luther University Halle-Wittenberg, Halle/Saale, Germany; [b]Institut Laue-Langevin (ILL), Grenoble, France

Key Words
Stratum corneum · Ceramide · Model membrane · Deuterium labelling · Neutron diffraction

Abstract
In order to elucidate the mode of action of the lipophilic penetration enhancer isopropyl myristate (IPM) on a molecular scale, we investigated oriented quaternary stratum corneum (SC) lipid model membranes based on ceramide AP, cholesterol, palmitic acid and cholesterol sulfate containing 10 wt% IPM by means of neutron diffraction. Our results indicate that IPM affects the lamellar lipid assembly in terms of bilayer perturbation and disordering. Phase segregation occurred, indicating that IPM is not likely to mix properly with the other SC lipids due to its branched structure. We used selective deuterium labelling to localize the penetration enhancer, and could successfully prove the presence of IPM in the two coexisting lamellar phases. We conclude that IPM's mode of action as penetration promoter is presumably based on incorporation into the SC lipid matrix, extraction of certain SC lipids into a separate phase and perturbation of the multilamellar lipid assembly.

Introduction

The protecting barrier properties of mammalian skin are generally accepted to be founded on the very thin outermost skin layer, the stratum corneum (SC). A highly ordered intercellular lipid matrix consisting of ceramides (CER), cholesterol (CHOL) with its derivatives and free fatty acids is arranged around protein-filled flat cells, the corneocytes. This coherent system substantially limits uncontrolled transepidermal water loss and prevents the unwanted absorption of substances [1, 2]. At the same time, those barrier properties can be obstructive for the dermal treatment of various skin diseases requiring a certain amount of drug to penetrate into skin. Acceleration of drug absorption can be facilitated by application of so-called penetration enhancers. Enhancer activity is presumably based on interaction with the SC lipid matrix and/or SC protein components, disordering or fluidizing effects on the SC lipids [3], and introduction of phase separation [4]. However, the exact mode of action is not yet fully elucidated on a molecular level. Synergetic effects in terms of drug flux enhancement have also been described, e.g. for myristic acid isopropyl ester (referred to as isopropyl myristate or IPM – a pharmaceutically used

KARGER

Fax +41 61 306 12 34
E-Mail karger@karger.ch
www.karger.com

1660–5527/12/0254–0200$38.00/0

Accessible online at:
www.karger.com/spp

Tanja Engelbrecht
Institute of Pharmacy, Martin Luther University Halle-Wittenberg
Wolfgang-Langenbeck-Strasse 4
DE–06120 Halle/Saale (Germany)
Tel. +49 345 552 5025, E-Mail tanja.engelbrecht@pharmazie.uni-halle.de

Table 1. Composition of the multilamellar SC lipid model membranes investigated by means of neutron diffraction

Sample	SC lipid components	wt%
Basic_IPM	CER[AP]/CHOL/PA/ChS/IPM	19.5/22.5/13.5/4.5/10
Basic_IPM-d_3	CER[AP]/CHOL/PA/ChS/IPM-d_3	19.5/22.5/13.5/4.5/10

liquid wax with well-established skin tolerability) in combination with alkanols [5, 6] and with propylene glycol [7]. Although it was also reported that IPM decreases hydrocortisone permeation through human skin [8], the ester is assumed to change the SC microstructure by insertion into the lipid lamellae where it is largely retained due to its high lipophilicity [5, 6]. Furthermore, the wax presumably liquefies the SC lipids due to its branched structure [7], which is supposed to account for the enhancer activity of IPM.

In recent years, the benefits offered by the neutron diffraction technique for the structural investigation of the SC lipid matrix in model membranes were highlighted in numerous works [9–11]. By using a simplistic model, the bilayer architecture of a membrane based on CER[AP], CHOL, palmitic acid (PA) and cholesterol sulfate (ChS) was revealed to be highly dependent on the phytosphingosine type CER[AP] which dictates the bilayer size due to its unique properties [12, 13]. A preceding study elucidated the mode of action of the penetration enhancer oleic acid on a molecular level [14]. It was shown that the position of lipid molecules within the model bilayers can be determined by specific deuterium labelling of molecular groups which can help shedding a light on the mode of enhancer activity on a molecular scale.

In the present work, we investigated the impact of IPM on the structure of a quaternary SC lipid model system based on CER[AP], CHOL, PA, and ChS which has been described before [13], containing either the protonated compound IPM (referred to as sample Basic_IPM) or the specifically deuterated compound IPM-d_3 which was received from chemical synthesis (sample Basic_IPM-d_3). In order to allow for a sufficient strength of the deuterium label to localize the enhancer, we decided to add an amount of 10 wt% IPM to the model membrane. The composition of the oriented multilamellar model membranes to be investigated by means of neutron diffraction can be found in table 1, and the chemical structures of the synthetic SC lipids used for sample preparation are displayed in figure 1. Local contrast enhancement by the deuterium label enabled us to directly localize the position of the liquid wax inside the membrane lipid lamellae.

Materials and Methods

CER[AP] [N-(α-hydroxyoctadecanoyl)-phytosphingosine] was generously provided by Evonik Goldschmidt GmbH (Essen, Germany). A chromatographic procedure using a silica gel column and chloroform/methanol gradient was applied to increase the purity of the substance above 96% before it was used. PA, CHOL, ChS, and tetradecanoic acid isopropyl ester (IPM) were purchased from Sigma Aldrich GmbH (Taufkirchen, Germany) and used as received. Specifically deuterated 14,14,14-d_3-tetradecanoic acid isopropyl ester (IPM-d_3) was received from own chemical synthesis [see Synthesis of 14,14,14-d_3-Tetradecanoic Acid Isopropyl Ester (IPM-d_3)]. All substances used for synthesis were purchased from Sigma Aldrich GmbH (Taufkirchen, Germany) except the deuterated compound, tetradecanoic acid-14,14,14-d_3, which was received from Larodan Fine Chemicals (Malmö, Sweden) and used without further purification. The product IPM-d_3 was purified by column chromatography using heptane/ether and gradient technique. The isopropanol was dried with sodium before use. All solvents were dried and distilled before use. Thionyl chloride was distilled twice at normal pressure. The ^{1}H NMR spectrum was recorded on a Varian Inova 500 apparatus (International Equipment Trading Ltd., Vernon Hills, Ill., USA, with an Oxford Instruments Ltd. superconducting magnet) at 27°C and $CDCl_3$ as internal standard. The mass spectrometric analysis was done using a Q-TOF1 mass spectrometer (Waters Micromass, Manchester, UK). The quartz slides (Spectrosil 2000, 25 × 65 × 0.3 mm) used for the neutron diffraction experiments were received from Saint-Gobain (Wiesbaden, Germany). An airbrush device (Harder & Steenbeck, Norderstedt, Germany) was employed to deposit the lipids onto the quartz surface. All buffer substances used were obtained from Sigma Aldrich.

For the preparation of oriented SC lipid model membranes to be investigated by neutron diffraction, we used a procedure according to the literature [15]. Appropriate amounts of the synthetic SC lipids dissolved in a mixture of chloroform/methanol (2:1 v/v) were combined. Twelve milligrams of the respective final SC lipid mixture (table 1) were sprayed onto the quartz surface using the airbrush device at constant air flow. The solvent was allowed to evaporate first under atmospheric pressure and subsequently under reduced pressure (<50 mbar), where the samples

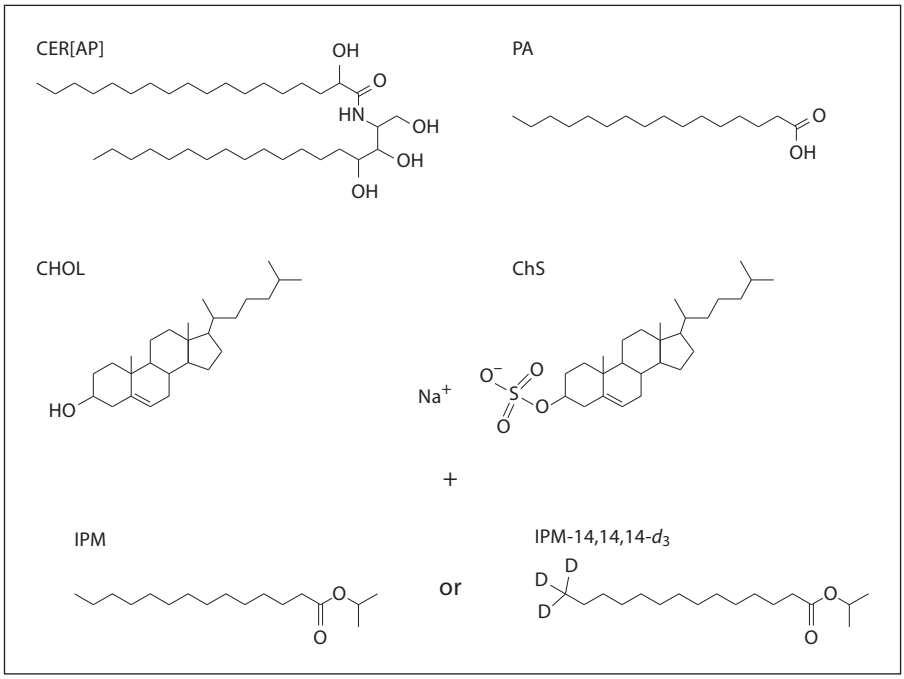

Fig. 1. The molecular structures of the synthetic SC lipids used for sample preparation.

were stored for 10–12 h. After the solvent was removed completely, a subsequent annealing procedure was applied, whereby the samples were heated to 75°C and cooled down to room temperature in water-saturated atmosphere. Subsequently, the samples were hydrated using a buffer solution of pH 9.6, for 5 min, and kept at room temperature until the diffraction measurements.

Synthesis of 14,14,14-d_3*-Tetradecanoic Acid Isopropyl Ester (IPM-*d_3*)*

0.43 mmol (100 mg) 14,14,14-d_3 tetradecanoic acid was suspended in 0.5 ml thionyl chloride. The mixture was allowed to stand overnight at room temperature. The excess of thionyl chloride was removed in vacuum. To the oily residue was dropped a mixture of 2.0 mmol (0.12 g) isopropanol and 0.2 mmol (0.16 g) dry pyridine, dissolved in 1 ml dry chloroform at 0°C over a period of 10 min with stirring. After a further hour at that temperature, the mixture was brought to room temperature and stirred for another hour. For workup, the solvent was removed in vacuum and the residue was purified by column chromatography with heptane and ether with a continuous increase of the polarity of the eluent. Yield: 120.4 mg, colorless oil, $C_{17}H_{31}D_3O_2$ (273.46). ^{1}H NMR (400 MHz, $CDCl_3$): δ = 1.19 (d, 6H, 2× [–CH_3]), 1.21–1.31 (m, 2H, [chain]), 1.55–1.63 (m, 2H, [–CH_2CH$_2$CO]), 2.2–2.25 (t, 2H, [–CH_2CO]), 4.98 (q, $^3J_{H,H}$ = 6.26, 1H, [–CH(CH$_3$)$_2$]). ESI-MS 274.27 [M$^+$]+H, 296.24 [M$^+$]+Na.

Neutron Diffraction Experiment

Neutron diffraction experiments were carried out using the small momentum transfer diffractometer D16 of the High-Flux Reactor at the Institut Laue-Langevin (Grenoble, France). The neutron wavelength λ was adjusted to 4.752 Å. The scattered neutron intensity was recorded during rocking scans (ω-scans, sample-to-detector distance: 95.0 cm) by the two-dimensional ^{3}He position-sensitive detector MILAND (area 320 × 320 mm, spatial resolution 1 × 1 mm). The samples were allowed to equilibrate before each measurement in lockable aluminium chambers at fixed temperature of 32°C and a relative humidity of 58%, achieved by a saturated aqueous solution of sodium bromide. Each sample was studied at three different D_2O concentrations in water (100/0, 50/50 and 8/92, v/v D_2O/H_2O) in order to vary the neutron scattering length density between the lipids and water. From a series of equidistant peaks, the spacing between the scattering planes (bilayer repeat distance d) was calculated using the correlation $d = 2 \times n \times \pi/Q_n$, where n is the diffraction order of the peak and Q_n is the scattering vector. The latter is correlated with the scattering angle 2θ by $Q = 4 \times \pi \times \sin\theta/\lambda$. Calculated d-spacings are presented in table 2.

Table 2. Calculated d spacings (in Å) for both samples investigated by means of neutron diffraction

Sample	Phase A	Phase B
Basic_IPM	46.8 ± 0.14	42.8 ± 0.6
Basic_IPM-d_3	45.9 ± 0.4	42.5 ± 0.43

For the interpretation of neutron diffraction data, commonly the neutron scattering length density profiles $\rho_s(x)$ are calculated by a Fourier synthesis of the structure factors F_h according to

$$\rho_s(x) = a + b\frac{2}{d} \times \sum_{h=1}^{h\ max} F_h \times \cos\left(\frac{2\pi hx}{d}\right)$$

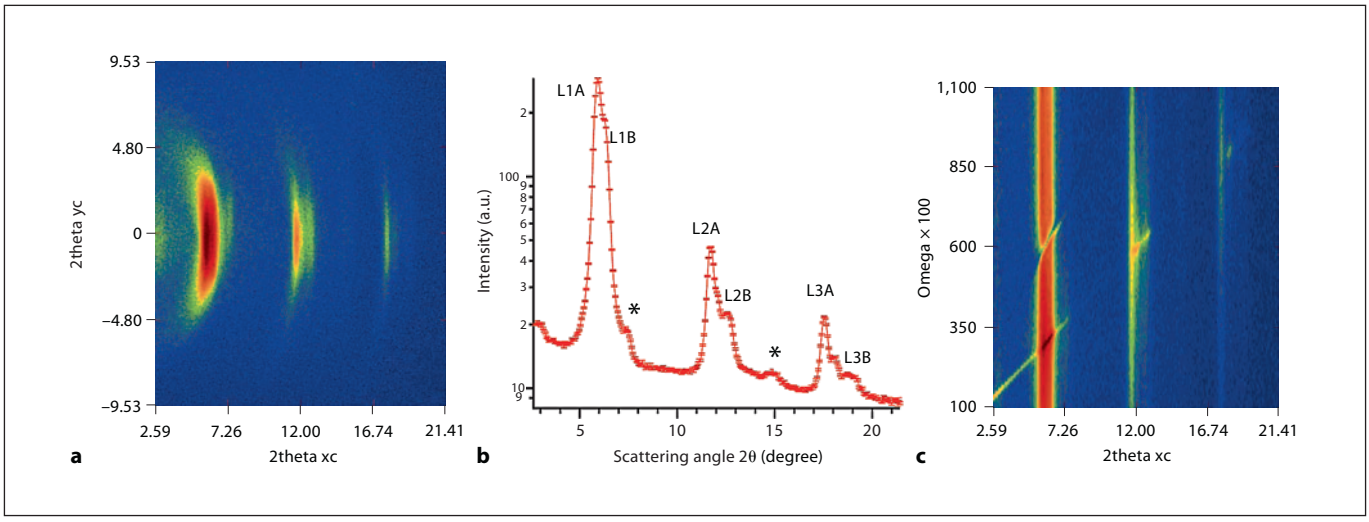

Fig. 2. Neutron diffraction pattern recorded at the first detector position for sample Basic_IPM at 32°C, 58% relative humidity, 100% D_2O. Shown are the 1st to 3rd Bragg reflections of phase A (L1A/L2A/L3A) and phase B (L1B/L2B/L3B), respectively. The first- and second-order diffraction peaks of phase-separated CHOL crystals (2theta = 7.49 and 14.84°) are marked with an asterisk in **b**. **a** Two-dimensional integrated intensity collected during an omega scan (sample rocking scan as shown in **c**). **b** Integrated intensity, plotted as log(I) versus 2theta. **c** Omega (ω) dependency of scattered neutron intensity (reciprocal space map).

The $\rho_s(x)$ represent the distribution of neutron scattering length density across one unit cell, i.e. one model bilayer, and therefore provide direct insight into the molecular arrangement of the SC lipids on a nanoscale. The phase of each F_h is determined by the isomorphous replacement method [16]. This is achieved by measuring each sample at least at three different D_2O/H_2O ratios.

The absolute value of F_h is received by

$$|F_h| = \sqrt{h \times I_h \times A_h},$$

where h is the Lorentz correction; A_h is the absorption correction and I_h is the integrated intensity of the hth peak. Data reduction to 2θ versus intensity I was performed with the Large Array Manipulation Program provided by the Institut Laue-Langevin [17], determination of the peak positions and intensities after background subtraction was performed using the software package IGOR Pro 6.1 (WaveMetrics Inc., Portland, Oreg., USA). A more detailed description of the neutron diffraction data evaluation can be found in the literature [18, 19].

Since neutrons are scattered by the atoms' nuclei and not by the electrons, the coherent neutron scattering length b_{coh} can differ markedly for different isotopes. According to the literature, b_{coh} for hydrogen (^1H) equals -0.374×10^{-12} cm and 0.667×10^{-12} cm for its isotope deuterium (^2H or D) [20]. Hence, it is possible to distinguish between protonated and deuterated compounds by means of neutron diffraction. For the localization of the deuterium label and therewith of the deuterated penetration enhancer IPM-d_3 inside the SC lipid model bilayers, the deuterium density distribution function $\rho_{diff}(x)$ was calculated as difference profile between the deuterated and the protonated sample: $\rho_{diff}(x) = \rho_{deut} - \rho_{prot}$. The maxima in the $\rho_{diff}(x)$ represent the position of the deuterium label within the unit cell.

Results and Discussion

The neutron diffraction pattern of sample Basic_IPM recorded at 32°C, 100% D_2O and 58% relative humidity is shown in figure 2b.

First, the neutron diffraction results reveal the occurrence of phase separation in the investigated model membranes containing 10 wt% IPM. Whereas the enhancer-free model membrane composed of CER[AP], CHOL, PA, and ChS was reported to feature a one-phase system [12, 13], the presence of the penetration enhancer obviously provokes the formation of two clearly pronounced and coexisting lamellar phases referred to as phase A and phase B. For reasons of simplicity, we will further refer to the enhancer-free quaternary model membrane lacking IPM as the reference system. In addition to the two lamellar phases, the 1st- and 2nd-order diffraction signals of crystalline CHOL were detected and are indicated with asterisks in figure 2b. The occurrence of such separate CHOL domains was described before and has been shown not to influence the bilayer assembly of SC lipid model systems [21, 22]. The lamellar repeat distances of the investigated samples were calculated as described above and are listed in table 2. In case of sample Basic_IPM, d equals 46.8 Å for phase A, and 42.8 Å for phase B, respectively. For sample Basic_IPM-d_3, the d spacings were determined as 45.9 Å (phase A) and 42.5 Å (phase B). There

is rather good agreement of the *d* spacings found for the present phase A (table 2) and the reference system of 45.6 Å being reported before [13]. Since just one component, IPM, was added to this model in the present study, it appears reasonable that phase A corresponds with the membrane structure reported for the reference system, and that furthermore the arrangement of the SC lipids in phase A is comparable to the reference system. In contrast, the lamellar spacing of phase B is comparatively smaller. We will refer to that later. Surprisingly, there is a small deviation for the lamellar repeat distance of phase A in sample Basic_IPM and sample Basic_IPM-d_3. Although the preparation procedures for both membranes were exactly the same, this experimental finding could indicate that there are slight variations in the lipid composition of phase A of both samples, e.g. a slightly higher or lower amount of CHOL and/or fatty acid and/or IPM. Yet the difference is quite small, therefore we regard phase A in both samples to be equivalent.

From these first results, we conclude that the membrane components are not likely to mix properly with each other in the presence of IPM. The branched structure of IPM with a highly mobile terminal isopropyl group probably prevents the other SC lipids to arrange in a densely packed and stable bilayer structure. Phase separation may further indicate that the solubility of the penetration enhancer IPM is limited in the lamellar 45.6-Å structure of the quaternary reference system which corresponds with the present phase A: after a certain limit value of IPM is exceeded, a fraction of the SC lipids is sequestered in the arising new lamellar structure. This emphasizes the impact of only 10% IPM added to the model membrane, and suggests that the enhancer indeed is incorporated into the bilayers and interacts with the SC lipids. To clarify whether IPM is localized in both phase A and phase B, or is accumulated in just one of the lamellar structures, the selectively deuterated IPM-d_3 was applied.

Furthermore, a distinct perturbation of the state of lamellar order was deduced from the shape of the neutron scattering signals in the diffraction pattern displayed in figure 2c. The Bragg sheet intensity is spread over a wider angular range in ω. This observation results from increased lamellar disorder in the model bilayers. Despite the still existing multilamellar assembly of the SC lipids, the bilayers seem to discover a certain perturbation. A possible explanation could be that the alkyl chains are no longer arranged in an *all-trans* zigzag structure, but exhibit an increased number of *gauche* defects. This is due to IPM, which is incorporated into the model bilayers but presumably requires more space due to its branched structure. The experimental finding of bilayer perturbation is in line with former reports [14], where a similar effect was observed after the addition of 10 wt% of the penetration enhancer oleic acid to the same quaternary model membrane as investigated here. Phase separation was not observed in this former work, but based on the findings the authors concluded that the introduction of *gauche* defects to the SC lipid alkyl chains and SC lipid bilayer perturbation considerably contribute to the enhancer activity of oleic acid [14].

Since the values of the *d* spacings are in the same order of magnitude for both model membranes studied here, further comparison between the samples Basic_IPM and Basic_IPM-d_3 was drawn. To gain insight into the bilayer architecture on a nanoscale and to prove the incorporation of IPM into the model bilayers, the neutron scattering length density profiles $\rho_s(x)$ were calculated for both samples and are comparatively displayed in figure 3 for phase A and phase B. Generally, both phases exhibit the typical $\rho_s(x)$ found for SC lipid bilayers. The two maxima that correspond with the hydrophilic bilayer region constituted by the SC lipid head groups are surrounding the lipid alkyl chains pointed towards the bilayer center, which is indicated by the central minimum. The difference profiles $\rho_{diff}(x)$ representing the density distribution of the deuterium label across the membrane are added. In comparison to the protonated SC model membrane (fig. 3), the curve progression for the deuterated sample is considerably lifted towards more positive values. This is observed for both, phase A and phase B, and arises from the presence of the d_3 label at the respective position within the membrane unit cell. We conclude from this finding that the deuterium label and therewith the enhancer IPM resides in both observed lamellar phases.

Yet, the *distribution* of the deuterium label itself appears to be different in both phases: whereas $\rho_{diff}(x)$ for phase B exhibits one maximum, three maxima are observed for phase A. This finding indicates that the arrangement of IPM is different within the two lamellar phases. Taking into account that all considerations regarding the molecular arrangement of the SC lipids in the present system are based on a centrosymmetric bilayer assembly, we interpret the diffraction results as follows. As expected from its molecular structure, a certain fraction of IPM points its myristoyl side chain towards the bilayer center, where the accumulation of positive neutron scattering length density due to the presence of three deuterium atoms at the chain end position causes the observed maximum in the $\rho_{diff}(x)$ around $x = 0$. Since the central

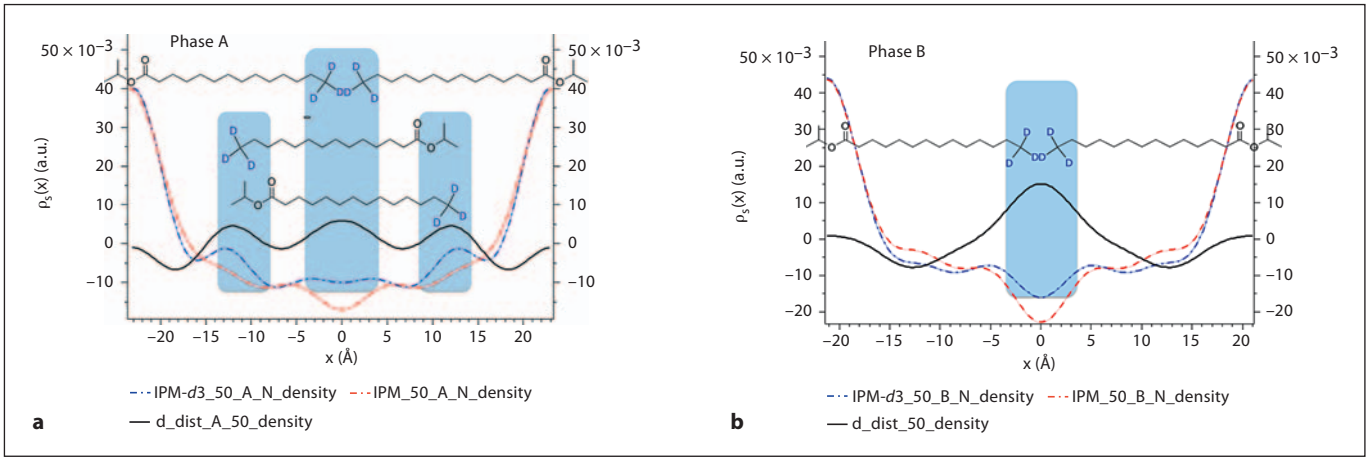

Fig. 3. a The neutron scattering length density profiles for phase A of sample Basic_IPM (red) and sample Basic_IPM-d_3 (blue) at 32°C and 50% D_2O. The difference profile or deuterium density distribution profile is presented as black solid line. For clarity, a sketch of the assumed arrangement of the penetration enhancer is added to the diagram. **b** The neutron scattering length density profiles for phase B of sample Basic_IPM (red) and sample Basic_IPM-d_3 (blue) at 32°C and 50% D_2O. The difference profile or deuterium density distribution profile is presented as black solid line. For better understanding, a sketch of two molecules IPM is added to illustrate the presumed enhancer arrangement. Colors refer to the online version only.

maximum is observed in both lamellar structures, this assembly of IPM is conceivable for both, phases A and B. For clarity, a sketch of the proposed assembly of two IPM molecules has been added to figure 3. Due to the hydrophobic match [23], the C14 chain of IPM will have high affinity to the C16 fatty acid (PA) present in the mixture and stretches through one hydrophobic bilayer leaflet. The more hydrophilic ester group most likely lies in the bilayer head group region, where hydrogen bonds with the other SC lipid head groups stabilize this arrangement. The isopropyl group would then be located near the hydrophilic bilayer region. Such an interaction of IPM and the SC intercellular lipid matrix has been proposed before [24]. Due to the limited number of structure factors F_h being available in the neutron diffraction experiment, the resolution of the Fourier synthesis is limited, which probably accounts for the comparatively broad dispersion of the maximum in the $\rho_{diff}(x)$ (fig. 3). The smeared-out maximum might also refer to a relatively broad distribution of the deuterium label itself inside the bilayers. As the C14 alkyl chain of IPM is slightly shortened compared to the C16 PA or the C18 chains of CER[AP], it seems likely that the terminal methyl group of IPM does not exactly reach the bilayer center, and that the CD_3 label therefore is localized slightly beside the position $x = 0$, as schematically presented in figure 3. Furthermore, since the presence of IPM was found to cause *gauche* defects and lamellar disorder, the alkyl chains will possess a certain mobility, which maybe results in a kind of delocalization of the deuterated label.

For phase A, the two additional maxima in the $\rho_{diff}(x)$ determined at the position of $|x| = 11.86 \pm 0.39$ Å suggest that a certain population of IPM is accommodated in the unit cell in a different way as explained above. Based on a centrosymmetric bilayer assembly, we regard both bilayer leaflets as mirrored equals. Surprisingly, the terminal methyl group with the deuterium label seems to be shifted away from the bilayer middle towards the region between center and head group moiety. To explain this observation, we assume that a fraction of the penetration enhancer might be inserted completely into the SC lipid bilayer, stretching the myristoyl chain through the bilayer center towards the neighbor bilayer leaflet, where the deuterated terminal methyl group is localized at the detected position of about 12 Å away from the bilayer center. Consequently, the ester group is no longer localized in the hydrophilic bilayer region, but has to integrate between the more hydrophobic alkyl chain moieties of the other SC lipids. Although this arrangement appears unexpected, such a complete incorporation into the SC lipid bilayers might be conceivable since IPM exhibits a comparatively high lipophilicity and is largely retained in the SC lipid matrix as highlighted before [6]. Moreover, a former neutron diffraction study revealed that CHOL is immersed in the bilayers of a quaternary model membrane in a similar way as proposed here for the molecule IPM,

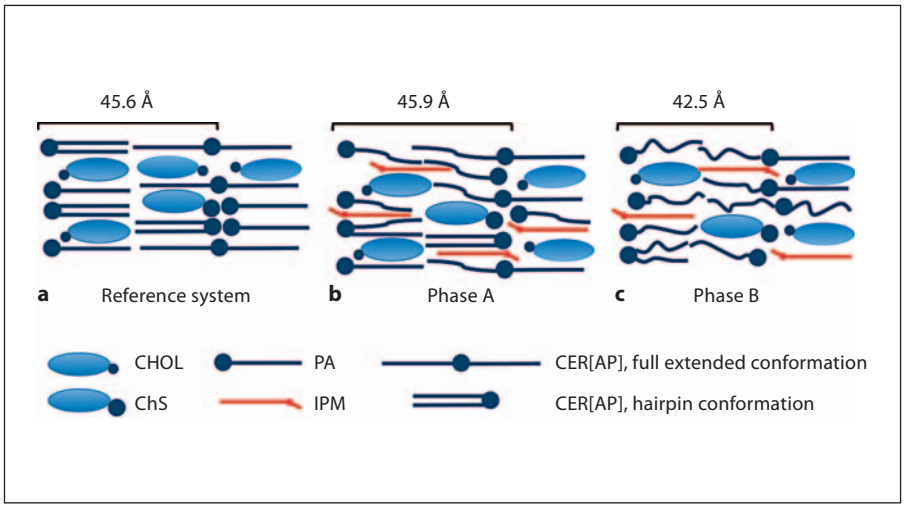

Color version available online

Fig. 4. Schematic presentation of the assumed lamellar structure in the presence of 10 wt% IPM-d_3. **a** Lamellar assembly of the components CER[AP], CHOL, PA and ChS in the short periodicity phase as reported in Kiselev et al. [13]. **b** The assumed bilayer structure of phase A. As described in the text, IPM can be either anchored with its ester group in the hydrophilic head group region, or completely inserted into the hydrophobic membrane region. The bilayer repeat distance is comparable to the quaternary reference system. Remarkable is the increased lamellar disorder. **c** The membrane structure and assembly of IPM in phase B. Note the decreased lamellar spacing, indicating an increased state of lipid fluidity and alkyl chain disorder.

with the hydrophilic OH group positioned inside the hydrophobic membrane region in order to allow for maximum hydrophobic interaction of the steroid ring system with the other membrane components [25]. Furthermore, the penetration enhancer IPM lacks a pronounced *hydrophilic head-hydrophobic tail* structure, for which reason the complete insertion – of at least few IPM molecules – might be possible. At this point, we have no definite explanation why only phase A shows two different arrangements for the penetration enhancer IPM, but it might be due to the larger spacing of phase A.

For a better understanding, the assumed structural assembly of the SC lipids in the two lamellar phases in the presence of IPM is schematically represented in figure 4 and compared to the bilayer nanostructure of the reference system. The latter has been extensively studied and described before [12, 13, 25]. It was shown that the driving force for the highly ordered nanostructure of the CER[AP]-based model membrane is the ceramide itself [13], and that the lamellar repeat distance remains stable even if the fatty acid is replaced by long-chain species [26]. Probably due to strong hydrogen bonds formed between the head groups of the CER molecules, a framework with a high state of lamellar order is built, and the other membrane components such as PA, CHOL and ChS are forced to arrange themselves inside the bilayers of short repeat distance of about 46 Å. We deduce that this bilayer structure is still intact after addition of 10 wt% IPM, since phase A exhibits a comparable repeat distance like reported for the reference system. Consequently, we conclude that CER[AP] remains to be the driving force for the formation of the bilayer structure, even in the presence of the penetration enhancer. Yet, the lamellar arrangement is strongly impaired and alkyl chain disorder is increased, as seen from the neutron diffraction signals. Selective deuteration proved that indeed, IPM is located in this phase A.

The occurrence of an additional phase indicates that a certain threshold of IPM may be exceeded, which separates together with other model membrane components in a new lamellar structure, phase B. The spacing of the latter is clearly decreased, which could further indicate that the presence of the enhancer causes a certain fluidization of the SC lipid alkyl chains arranged in this phase. This leads to stronger interdigitation of the other SC lipids and consequently to a decrease in the lamellar spacing [27]. Moreover, one could speculate that the bilayer-stabilizing impact of CER[AP] is reduced in phase B, maybe due to a slightly smaller amount of CER being present in this newly formed lamellar structure. A bilayer structure altered in such a way with increasingly disordered alkyl chains due to the presence of IPM would consequently offer a diminished resistance against drug flux and could provide an optimal route for the drug molecules traversing the skin barrier. With regard to the mechanism of the enhancer activity of IPM, it is therefore conceivable that the incorporation of IPM together with its significant bilayer disordering effects strongly contribute to IPM's ability to increase drug flux through the skin. It was already suggested by Brinkmann and Mueller-Goymann [24] that IPM is inserted into the SC lipid bilayers with the isopropyl group anchored in the polar region and the myristoyl chain pointing towards the bilayer center. The present results corroborate the assumption of such an arrangement of IPM. In addition, our study suggests that

IPM might also be completely immersed into the SC lipid bilayers, and that IPM causes phase separation in an oriented quaternary SC lipid model based on CER[AP]. The stabilizing influence of the ceramide present in the membrane seems to be outbalanced by the perturbing effect of the penetration enhancer.

In conclusion, we successfully localized the deuterium-labelled penetration enhancer and could therewith prove the incorporation of IPM into the SC lipid model membrane. In the presence of the lipophilic penetration enhancer IPM, a dense lamellar arrangement of all membrane components in a single phase is hindered. Our results provide direct evidence that IPM's mode of action as penetration enhancer results from affecting the bilayer architecture of the SC lipids, by introducing phase separation, and by direct perturbation of a proper lamellar arrangement.

Acknowledgements

We thank Evonik Goldschmidt GmbH (Essen, Germany) for the donation of CER[AP]. T.N.E. thanks Evonik Goldschmidt GmbH and the Graduiertenförderung des Landes Sachsen-Anhalt for funding. Granting of beam time and financial assistance by Institut Laue-Langevin (Grenoble, France) is gratefully acknowledged.

References

1 Elias PM: Epidermal lipids, membranes, and keratinization. Int J Dermatol 1981;20:1–19.
2 Potts RO, Francoeur ML: The influence of stratum corneum morphology on water permeability. J Invest Dermatol 1991;96:495–499.
3 Barry BW, Bennett SL: Effect of penetration enhancers on the permeation of mannitol, hydrocortisone and progesterone through human skin. J Pharm Pharmacol 1987;39:535–546.
4 Ongpipattanakul B, Burnette RR, Potts RO, Francoeur ML: Evidence that oleic acid exists in a separate phase within stratum corneum lipids. Pharm Res 1991;8:350–354.
5 Goldberg-Cettina M, Liu P, Nightingale J, Kurihara-Bergstrom T: Enhanced transdermal delivery of estradiol in vitro using binary vehicles of isopropyl myristate and short-chain alkanols. Int J Pharm 1995;114:237–245.
6 Müller-Goymann CC, Mitriaikina S: Synergetic effects of isopropyl alcohol (IPA) and isopropyl myristate (IPM) on the permeation of betamethasone-17-valerate from semisolid pharmacopoeia bases. J Drug Delivery Sci Technol 2007;17:339–346.
7 Arellano A, Santoyo S, Martin C, Ygartua P: Influence of propylene glycol and isopropyl myristate on the in vitro percutaneous penetration of diclofenac sodium from carbopol gels. Eur J Pharm Sci 1998;7:129–135.
8 Brinkmann I, Mueller-Goymann CC: Role of isopropyl myristate, isopropyl alcohol and a combination of both in hydrocortisone permeation across the human stratum corneum. Skin Pharmacol Appl Skin Physiol 2003;16:393–404.
9 Engelbrecht T, Hauss T, Suss K, Vogel A, Roark M, Feller SE, Neubert RHH, Dobner B: Characterisation of a new ceramide EOS species: synthesis and investigation of the thermotropic phase behaviour and influence on the bilayer architecture of stratum corneum lipid model membranes. Soft Matter 2011;7:8998–9011.
10 Groen D, Gooris GS, Barlow DJ, Lawrence MJ, van Mechelen JB, Deme B, Bouwstra JA: Disposition of ceramide in model lipid membranes determined by neutron diffraction. Biophys J 2011;100:1481–1489.
11 Schröter A, Kessner D, Kiselev MA, Hauss T, Dante S, Neubert RHH: Basic nanostructure of stratum corneum lipid matrices based on ceramides [EOS] and [AP]: a neutron diffraction study. Biophys J 2009;97:1104–1114.
12 Kiselev MA: Conformation of ceramide 6 molecules and chain-flip transitions in the lipid matrix of the outermost layer of mammalian skin, the stratum corneum. Crystallogr Rep 2007;52:525–528.
13 Kiselev MA, Ryabova NY, Balagurov AM, Dante S, Hauss T, Zbytovská J, Wartewig S, Neubert RHH: New insights into the structure and hydration of a stratum corneum lipid model membrane by neutron diffraction. Eur Biophys J 2005;34:1030–1040.
14 Engelbrecht TN, Schroeter A, Hauss T, Neubert RH: Lipophilic penetration enhancers and their impact to the bilayer structure of stratum corneum lipid model membranes: neutron diffraction studies based on the example oleic acid. Biochim Biophys Acta 2011;1808:2798–2806.
15 Seul M, Sammon MJ: Preparation of surfactant multilayer films on solid substrates by deposition from organic solution. Thin Solid Films 1990;185:287–305.
16 Franks NP, Lieb WR: Structure of lipid bilayers and the effects of general anaesthetics: an X-ray and neutron diffraction study. J Mol Biol 1979;133:469–500.
17 Richard D, Ferrand M, Kearley GJ: Analysis and visualisation of neutron-scattering data. J Neutron Res 1996;4:33–39.
18 Nagle JF, Tristram-Nagle S: Structure of lipid bilayers. Biochim Biophys Acta 2000;1469:159–195.
19 Worcester DL, Franks NP: Structural analysis of hydrated egg lecithin and cholesterol bilayers. 2. Neutron diffraction. J Mol Biol 1976;100:359–378.
20 Sears VF: Neutron scattering lengths and cross sections. Neutron News 1992;3:26–37.
21 Ali MR, Cheng KH, Huang J: Ceramide drives cholesterol out of the ordered lipid bilayer phase into the crystal phase in 1-palmitoyl-2-oleoyl-sn-glycero-3-phosphocholine/cholesterol/ceramide ternary mixtures. Biochemistry 2006;45:12629–12638.
22 Pata V, Dan N: Effect of membrane characteristics on phase separation and domain formation in cholesterol-lipid mixtures. Biophys J 2005;88:916–924.
23 Ouimet J, Lafleur M: Hydrophobic match between cholesterol and saturated fatty acid is required for the formation of lamellar liquid ordered phases. Langmuir 2004;20:7474–7481.
24 Brinkmann I, Mueller-Goymann CC: An attempt to clarify the influence of glycerol, propylene glycol, isopropyl myristate and a combination of propylene glycol and isopropyl myristate on human stratum corneum. Pharmazie 2005;60:215–220.
25 Kessner D, Kiselev MA, Hauss T, Dante S, Wartewig S, Neubert RH: Localisation of partially deuterated cholesterol in quaternary SC lipid model membranes: a neutron diffraction study. Eur Biophys J 2008;37:1051–1057.
26 Ruettinger A, Kiselev MA, Hauss T, Dante S, Balagurov AM, Neubert RH: Fatty acid interdigitation in stratum corneum model membranes: a neutron diffraction study. Eur Biophys J 2008;37:759–771.
27 Zhang RT, Sun WJ, Tristramnagle S, Headrick RL, Suter RM, Nagle JF: Critical fluctuations in membranes. Phys Rev Lett 1995;74:2832–2835.